

ALMA MEMO No. 535
Simulation Series of a Phase Calibration Scheme
with Water Vapor Radiometers for the Atacama Compact Array

Yoshiharu Asaki (ISAS),
Masao Saito (NAOJ), Ryohei Kawabe (NAOJ),
Koh-ichiro Morita (NAOJ), Youichi Tamura (Univ. of Tokyo/NAOJ), and
Baltasar Vila-Vilaro (NAOJ)

September 8, 2005

Abstract

We have carried out a series of simulations of a phase calibration scheme for the Atacama Compact Array (ACA) ¹ using water vapor radiometers (WVRs). **In the proposed scheme the WVRs devoted to measurements of tropospheric water vapor content are attached to the 12-m antennas.** The excess path length (EPL) due to the tropospheric water vapor variations aloft is fitted to a simple two-dimensional slope using WVR measurements. Interferometric phase fluctuations for each baseline due to the turbulent water vapor are obtained from differences of inferred line-of-sight EPL and subtracted from the interferometric phases for the correction. We have estimated residual root-mean-square (RMS) phases for 30-m baselines after the correction for various values of WVR measurement errors, wind velocities, coefficients and power-law exponents of the spatial structure function of the EPL, and extents of the distribution of the WVR instruments. From the simulations we found that, for WVRs with no measurement errors, the proposed calibration scheme shows an excellent performance for all tropospheric conditions, and that a simple relationship between the residual RMS phase and the extent of the WVR distribution exists: the closer the extent to the interferometer array is, the more effective the calibration scheme will be. When WVR measurement errors are added, although the RMS phases are still improved in unstable tropospheric conditions (50-percentile conditions), the proposed calibration scheme may not be needed in good conditions (25-percentile conditions). We found that, if the performance of the WVR achieves the expected level (a factor of about three better than the current ALMA WVR specification), the proposed scheme is quite promising for the ACA. In addition, we provided a simple statistical model to explain the simulation results. The simulations and the following analyses with the statistical model show that radio seeing data with baselines of 10–30 m is important to determine the optimum extent of the WVR distribution around the interferometer array. Monitoring of the radio seeing as well as the WVR measurement errors during observations will be useful to judge whether pre-calibrated data with the proposed calibration scheme should be used in the following ACA data reduction or not. For observations at lower elevations made by the ACA, the expected performance of the WVR is also important.

¹ The ACA consists of twelve 7-m antennas for interferometry and four 12-m antennas to measure total power of celestial sources.

1 Introduction

The Atacama Compact Array (ACA) is designed to improve the short baseline coverage of the Atacama Large Millimeter Array (ALMA) especially for observations of extended radio structures. The ACA consists of twelve 7-m antennas for interferometry and four 12-m antennas for total power measurements of celestial sources. *Tsutsumi et al.* (2004) showed in their imaging simulations that atmospheric phase fluctuations play a major role in synthesizing the visibilities with the ALMA including the ACA. Effective phase calibration schemes for the ACA should be carefully discussed because the array configuration of the ACA is so compact that the fast switching phase calibration will not work effectively (*Holdaway, 2004(b)*).

Here we propose a phase calibration scheme in which a simple two-dimensional (2-D) slope of the excess path length (EPL) due to tropospheric water vapor variations aloft is determined from measurements with water vapor radiometers (WVRs) attached to the four 12-m single-dish antennas located nearby to the ACA 7-m interferometer array. The fitted surface is used to obtain line-of-sight EPL values for each individual antenna of the interferometer array. Interferometric phase fluctuations due to the water vapor for each interferometer baseline are estimated from the differences of the obtained EPL between the 7-m antennas. The interferometric phases of each baseline of the ACA are then calibrated by subtracting the differences. Here we present a feasibility study on how effective the proposed calibration scheme is for the ACA, and studies on what the most effective configuration of the single-dish antennas is, and what parameters of the tropospheric spatial structure function (SSF) affect residual root-mean-square (RMS) phases after the correction. To answer those questions we have carried out a series of simulations based on a tropospheric water vapor distribution as a phase screen assuming frozen flow (*Dravskikh and Finkelstein, 1979*). In section 2 we describe the simulation parameters of the phase screen and array configurations. We present the simulation results in section 3. We discuss the results, using a simple statistical model, in section 4. In section 5 we summarize the results. **All the phase fluctuations mentioned in this memo are in path length.**

2 Simulation Parameters

2.1 Phase Screen and Frozen Flow

In the present simulations the tropospheric water vapor distribution is modeled as a phase screen assuming frozen flow. This simple model is very useful in considering the interferometric phase fluctuations due to the troposphere (*Asaki et al., 1996; Asaki et al., 1998*), although it should be noted that such a simple structure is not always observed (*Beaupuits et al., 2005*). In the software developed for these simulations, the phase screen is generated to cover the whole extent of the array. The screen in the simulations keeps the distribution pattern of the water vapor and flows at a wind velocity v_w along an arbitrary direction. The grid interval of the screen is set to 1 meter in the simulated screen. According to *Dravskikh and Finkelstein (1979)* the SSF of the tropospheric path length, D , can be expressed as follows:

$$D(\rho) = C^2 \rho^{2\alpha} \quad (\rho \leq L_1), \quad (1)$$

$$D(\rho) = C^2 L_1^{\alpha - \frac{2}{3}} \rho^{\frac{2}{3}} \quad (L_1 < \rho \leq L_2), \quad (2)$$

$$D(\rho) = C^2 L_1^{\alpha - \frac{2}{3}} L_2^{\frac{2}{3}} \quad (\rho > L_2), \quad (3)$$

where ρ is a spatial distance, L_1 and L_2 are an inner and outer scale of the phase screen, respectively,

α is one half of the structure exponent, and C is a structure coefficient of the inner scale. The inner and outer scales are typically considered to be 1 and 10 km, respectively, and *Carilli and Holdaway* (1999) observationally showed the inner and outer scale of 1.2 and 6 km at the VLA site. Since in the simulation software the scales can be selected among $2^n \times$ (grid interval) where n is an integer number, those scales are fixed to 1024 and 8192 m for the inner and outer scale, respectively. We used the structure exponent of 1.16 (*Holdaway, 2004(a)*), and 1.67 (Kolmogorov turbulence) in these simulations. The structure coefficient was set to have values of $\sqrt{D(\rho = 100 \text{ m})} = 25, 50, \text{ and } 100 \mu\text{m}$ in path length. The last two values are very close to the 25- and 50-percentile tropospheric conditions at Chajnantor, assuming the structure exponent of 1.16. The parameters used in the simulations are listed in Table 1. Note that, since we set the observing direction to the zenith in the simulations, the results reported here are independent of the altitude of the screen. An example of the generated phase screen is shown in Figure 1.

2.2 Geometry of Interferometer Antennas and Water Vapor Radiometers

The geometry of the antennas and the phase screen are shown in Figure 2. There are two groups in the array: one, referred as the “interferometer array”, has four 7-m interferometer antennas, the other one, referred as the “total-power array” has the 12-m diameter antennas to which the WVRs are attached. The interferometer array is laid out as two 30-m baselines, one North-South and one East-West. The configuration of the interferometer array is fixed in all the simulations. The 12-m antennas of the total-power array are set on the four corners of a square surrounding the interferometer array. The antennas of the total-power array are used to detect the water vapor content at the zenith. We selected three configurations of the total-power array of $30 \text{ m} \times 30 \text{ m}$, $50 \text{ m} \times 50 \text{ m}$, and $50 \text{ m} \times 70 \text{ m}$ as shown in Figure 3. We label them array 1, 2, and 3, respectively. In the simulations we assume that all the antennas have a uniform illumination pattern, and that the phase screen is in the near field of the antennas.

2.3 Data Accumulation and Phase Correction

The interferometric phase fluctuations of the interferometer array are generated in three steps. The first step is to average the grid data of the EPL phase screen within the 7-m diameter cylindrical beam projected on the phase screen in every 0.1 sec. The frozen screen moves a distance of $v_w/10$ meters from West to East during a single average sample. The second step is to compute the differences of the spatially averaged path lengths between the antennas in the array. The final step is to average ten consecutive differences per baseline to make a one-second averaged interferometric phase in path length.

The data accumulation of the WVR consists of two steps. The first step is to average the grid data within the 12-m diameter cylindrical beam. The next step is to average ten of these to make a one-second averaged WVR measurement in path length. As we mention later, we have performed simulations assuming both errorless WVRs and realistic ones with current noise estimates in *Hills* (2004). For the latter, random Gaussian noise with a standard deviation σ_{wvr} of 7 or 25 μm for one-second integration is added to the one-second EPL data. The former value of the error comes from the expected performance of the WVR devices as shown in Figure 1 in ALMA Memo No.495 (*Hills, 2004*), while the latter one is the ALMA WVR performance specification for a 1.5-mm of precipitable water vapor (PWV) calculated as follows,

$$\sigma_{\text{wvr}} = 10 (1 + \text{PWV}[\text{mm}]) \text{ } [\mu\text{m}]. \quad (4)$$

The phase calibration has four steps. In the first step the EPL 2-D slope fitting is carried out every one second with the WVR measurements. The next step is to infer the line-of-sight EPLs of the interferometer antennas from the normal unit vector of the slope and the EPL bias at the center of the total-power array. In the third step the interferometric phase fluctuations for each baseline are estimated from the differences of the inferred line-of-sight EPLs for each pair of antennas. In the last step the interferometric phases are then calibrated by subtracting the values in the previous step. Examples of the WVR 2-D slope fitting are shown in Figure 1.

Each simulation is 600 seconds long, to estimate the residual RMS phase of the interferometric baselines after the correction. A set of ten of these simulations with the same set of the parameters is run to obtain statistically reliable results. In the simulations all the statistical values are processed in path length.

3 Results

Simulation results for the case when no phase correction (the so-called natural seeing), and with the proposed phase calibration are shown in Figures 4 and 5, respectively. Since, as can be seen in the plots, there is not much difference in the results for wind velocities of 5 and 10 m/s, we will not discuss the wind velocity any more.

When the WVR measurement errors are not considered, we found that the proposed calibration scheme shows an excellent performance for all the tropospheric conditions. The residual RMS phases after the correction decrease as the extent of the total-power array is getting closer to the interferometer array. This result seems to be natural, as in the case that the most effective total-power array should have the same configuration of the interferometer array. When WVR measurement errors are added, the residual RMS phases are still improved with the proposed phase calibration for situations with larger tropospheric phase fluctuations (unstable tropospheric conditions, or 50-percentile tropospheric conditions). The simulations also show that, for the smaller phase fluctuations (stable tropospheric conditions), an application of the proposed scheme makes the interferometer phase fluctuations worse than the natural seeing, especially for the WVR measurement error of $25 \mu\text{m}$ in EPL (ALMA specifications for the WVR with 1.5-mm PWV). This is because the WVR measurement error is getting larger than the amplitude of the natural seeing for good tropospheric conditions. In such cases the WVR phase calibration should not be applied to the ACA. On the other hand, for a WVR measurement error of $7 \mu\text{m}$, which is a factor of about three better than the current ALMA WVR specification, the proposed scheme is quite promising for the ACA phase calibration for most tropospheric conditions. According to *Hills* (2004), such a high WVR performance can be expected.

There are clear differences between structure exponents of 1.16 and 1.67. These differences are caused by both the exponent and the natural seeing value for a 30-m spatial separation. Since the interferometric phase fluctuations decrease more rapidly in the case of Kolmogorov turbulence (ie, $\alpha = 0.87$) as the baseline is getting shorter, the residual RMS phases of a 30-m baseline in the Kolmogorov case is smaller than the other for the same fluctuation amplitude at $\rho = 100$ m. Knowledge of the SSF characteristics for spatial scales less than several tens of meters is fundamental for the ACA, and it is clear from this work that the statistics of the SSF of 10–30 m is very important for the ACA phase calibration. Radio seeing data with short range baselines as well as the WVR measurement errors will be a useful guideline to judge whether pre-calibrated data with the proposed calibration scheme should be used in the following ACA data reduction or not.

4 Discussion

4.1 Statistical model

The simulations mentioned above are very helpful for us to investigate the feasibility of the proposed calibration scheme. To find out the optimum configuration of the total-power array we have used simple statistical models to ascertain which errors affect the proposed calibration scheme most. Here we estimate the calibrated residual RMS phases with a one-dimensional (1-D) slope fitting system with two WVRs and a single interferometric baseline as shown in Figure 6. In the following discussion, we will not take into account either the smoothing effects of the antenna aperture or one-second averaging of the EPL for the sake of simplicity.

We consider two error sources in the proposed scheme: one is the influence of the WVR measurement errors in the slope fitting (σ_{fit}), and the other is due to the minor fluctuations not corrected by our simple 1-D slope fit (σ_{trp}). The former error, σ_{fit} , in the 1-D slope fitting can be expressed using the WVR measurement error, σ_{wvr} , as follows:

$$\sigma_{\text{fit}} = \frac{\sqrt{2}r}{R}\sigma_{\text{wvr}}, \quad (5)$$

where R is the separation between the WVRs, and r is the baseline length of the interferometer. The latter error, σ_{trp} , can be expressed using the SSF as follows:

$$\begin{aligned} \sigma_{\text{trp}}^2 &= \left\langle \left\{ \left[\Phi \left(d + \frac{R+r}{r} \right) - \Phi \left(d + \frac{R-r}{r} \right) \right] - \frac{r}{R} [\Phi(d+R) - \Phi(d)] \right\}^2 \right\rangle \\ &= D(r) + \left(\frac{r}{R} \right)^2 D(R) + \frac{2r}{R} \left\{ D \left(\frac{|R-r|}{2} \right) - D \left(\frac{R+r}{2} \right) \right\}, \end{aligned} \quad (6)$$

where Φ is the tropospheric phase fluctuations in path length, and d is a reference position. The total error, σ_{total} , can be expressed as follows:

$$\sigma_{\text{total}} = \sqrt{\sigma_{\text{fit}}^2 + \sigma_{\text{trp}}^2} \quad . \quad (7)$$

On the other hand, the natural seeing can be estimated by $\sqrt{D(r)}$. Figure 7 shows statistical estimations of the residual RMS phases using equations (5), (6), and (7) for $R = 50$ m, $r = 30$ m, and $\sigma_{\text{wvr}} = 7$ or $25 \mu\text{m}$. We obtained very similar results to those already shown in Figure 5. These new plots clearly show that our calibration scheme requires the WVR errors to be as small as possible.

Figure 8 shows statistical estimations of the residual RMS phases after correction for various values of R . In the case of $\sigma_{\text{wvr}} = 7 \mu\text{m}$, the minimum of the residual RMS phase is obtained with $R = r$ for unstable tropospheric conditions (for instance, $\sqrt{D(\rho = 100 \text{ m})} = 100 \mu\text{m}$ and $\alpha = 0.58$). On the other hand, for stable conditions (for instance, $\sqrt{D(\rho = 100 \text{ m})} = 25 \mu\text{m}$ and $\alpha = 0.58$), the residual RMS phases are not strongly dependent on the closeness between the interferometer and total-power array for $R > r$. This trend can also be seen in the simulation results in the previous section. This is mainly because the influence of the WVR measurement errors is getting relatively larger on the fitting for the shorter baseline of the total-power array as indicated in equation (5), especially for stable tropospheric conditions. Statistics of the radio seeing data with spatial scales less than several tens of meters will be valuable to determine the optimum configuration of the total-power array from the viewpoint of the phase calibration.

4.2 Effectiveness at low elevations

Since the ACA will need to observe four times longer than the ALMA to reach the same sensitivity on the same source, the ACA will have to cover lower elevations than the ALMA. Therefore, it is interesting to investigate the effectiveness of the proposed scheme for the ACA at lower elevations. Using the statistical model mentioned above, we now consider the effectiveness of the proposed scheme at low elevations. Here we consider the case of an elevation angle of 30° (zenith angle of 60°).

Numerical calculations based on an analytical model of the tropospheric phase fluctuations with the assumption of Kolmogorov turbulence indicate that the tropospheric SSF has an elevation dependence (*Treuhaft and Lanyi, 1987*). According to this model, σ_{trp} can be modified as follows:

$$\sigma'_{\text{trp}} = \sqrt{\sec Z} \sigma_{\text{trp}}, \quad (8)$$

where Z is the zenith angle. At $Z = 60^\circ$ the height of the column of water condensed along the line-of-sight is 3 mm when the zenith PWV is 1.5 mm. The WVR measurement error of the ALMA WVR specification can be calculated as $40 \mu\text{m}$ using equation (1). The expected performance of the WVR at $Z = 60^\circ$ is $13 \mu\text{m}$ in the measurement error from Figure 1 in ALMA Memo No.495 (*Hills, 2004*). Figure 9 shows statistical estimations of the residual RMS phases in the case of $Z = 60^\circ$ for $R = 50 \text{ m}$, and $r = 30 \text{ m}$. The residual RMS phases are improved compared with the natural seeing at the zenith angle of 60° , and it can be expected from our analysis to make the residual RMS phases smaller than the ALMA specification of the path length fluctuations at lower elevations. Since the natural seeing at $Z = 60^\circ$ increases with the atmospheric phase fluctuations more rapidly, the expected WVR performance introduced by *Hills (2004)* is also important for the proposed phase calibration scheme for observations at lower elevation coverage made by the ACA in stable tropospheric conditions.

5 Summary

We reported here simulations of a new phase calibration scheme proposed for the ACA in which a simple 2-D slope of the EPL due to the tropospheric water vapor variations is determined with measurements with WVRs attached to 12-m single-dish antennas located nearby to the ACA 7-m interferometer array. We also provided a simple 1-D statistical model of the calibration scheme that can explain the results. Though this simple statistical model cannot reproduce the simulation results completely, especially when the baselines of the interferometer array are not aligned with those of the total-power array, the residual RMS phases can still be inferred with this simple model well.

The simulations in this memo showed that the proposed scheme is quite promising for the ACA phase calibration even at lower elevations if the expected WVR performance (a factor of a few better than the current ALMA specification of the WVR) can be achieved. On the other hand, when the WVR measurement error is equivalent to the ALMA WVR specifications, the proposed scheme has a problem that the calibrated phase fluctuates more than the natural seeing for good tropospheric conditions. For the ALMA WVRs, our results suggest that the smaller the WVR measurement errors the better, thus guaranteeing that they are quite smaller than the current ALMA WVR specification is critical. We also showed that the expected WVR performance is quite important for ACA observations with the proposed calibration scheme.

Radio seeing data with baselines of 10–30 m are important to determine the optimum extent of the total-power array because wider distributions of the WVRs seem to have an advantage over the compact distributions for the stable tropospheric conditions, while the closer WVR distributions will be better in the unstable tropospheric conditions. Since the proposed phase calibration scheme with

the realistic WVRs may not be needed for the ACA in very good tropospheric conditions, monitoring of the radio seeing as well as the WVR measurement errors during observations will be important to judge whether pre-calibrated data with the proposed calibration scheme should be used in the following ACA data reduction or not.

References

- Asaki, Y., M. Saito, R. Kawabe, K-I. Morita, and T. Sasao, *Radio Sci.*, *31*, 1615-1625, 1996.
- Asaki, Y., K. M. Shibata, R. Kawabe, D-G. Roh, M. Saito, K-I. Morita, and T. Sasao, *Radio Sci.*, *33*, 1297-1318, 1998.
- Beaupuits, J. P. P., R. C. Rivera, and L-Å. Nyman, ALMA memo, in preparation.
- Carilli, C. L., and M. A. Holdaway, *Radio Sci.*, *34*, 817-840, 1999.
- Dravskikh, A. F., and A. M. Finkelstein, *Astrophys.Space Sci.*, *60*, 251-265, 1979.
- Hills, R., ALMA memo 495, 2004.
- Holdaway, M., ALMA memo 490, 2004(a).
- Holdaway, M., ALMA memo 491, 2004(b).
- Treuhaft, R. N., and G. E. Lanyi, *Radio Sci.*, *22*, 251-265, 1987.
- Tsutsumi, T., K-I. Morita, T. Hasegawa, and J. Pety, ALMA memo 488.1, 2004.

Altitude of the screen	1 km
Mean Value of PWV (zenith)	1.5 mm
Wind direction	West to East
Wind velocity	5, 10 m/s
Path Length Fluctuation (100-m spatial separation)	25, 50, 100 μm
Structure Exponent of SSF (inner scale)	1.16, 1.67
Grid interval of the phase screen	1 m
WVR measurement error	0, 7, 25 μm

Table 1: Parameters used in the simulations.

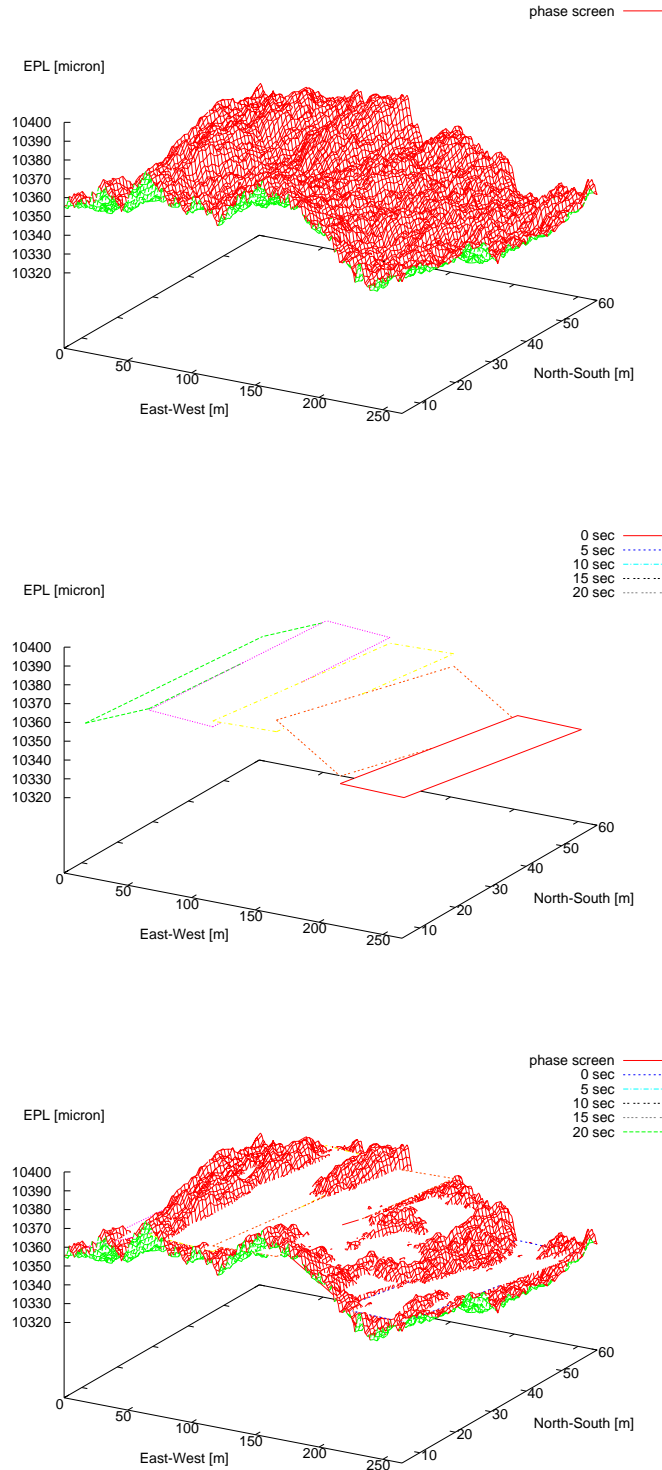


Figure 1: Examples of the 2-D slope fitting in the simulations for the total-power array of $50 \text{ m} \times 50 \text{ m}$. The WVR measurement errors are not included. The top plot shows a generated EPL phase screen ($300 \text{ m} \times 50 \text{ m}$) moving with the wind velocity of 10 m/s , the middle one shows the fitting results with the four WVRs attached to the 12-m antennas, and the bottom one shows the superposition of the screen and the fitted planes.

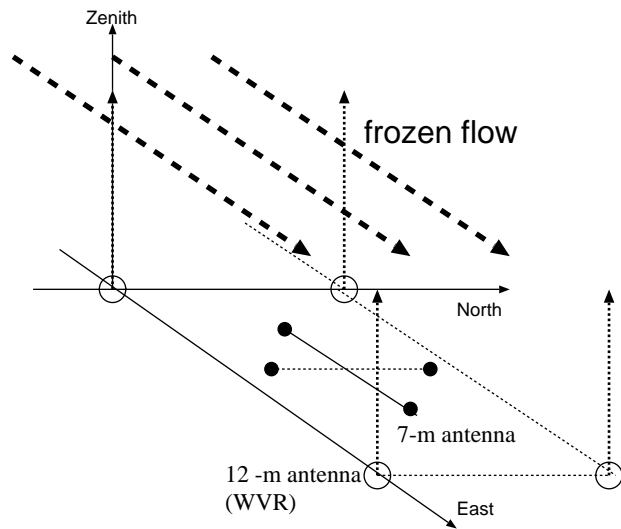


Figure 2: Schematic diagram of the geometry of the simulated array and phase screen. Large open circles represent the 12-m diameter antennas to measure the EPL. Small filled circles represent the 7-m diameter antennas of the interferometer array.

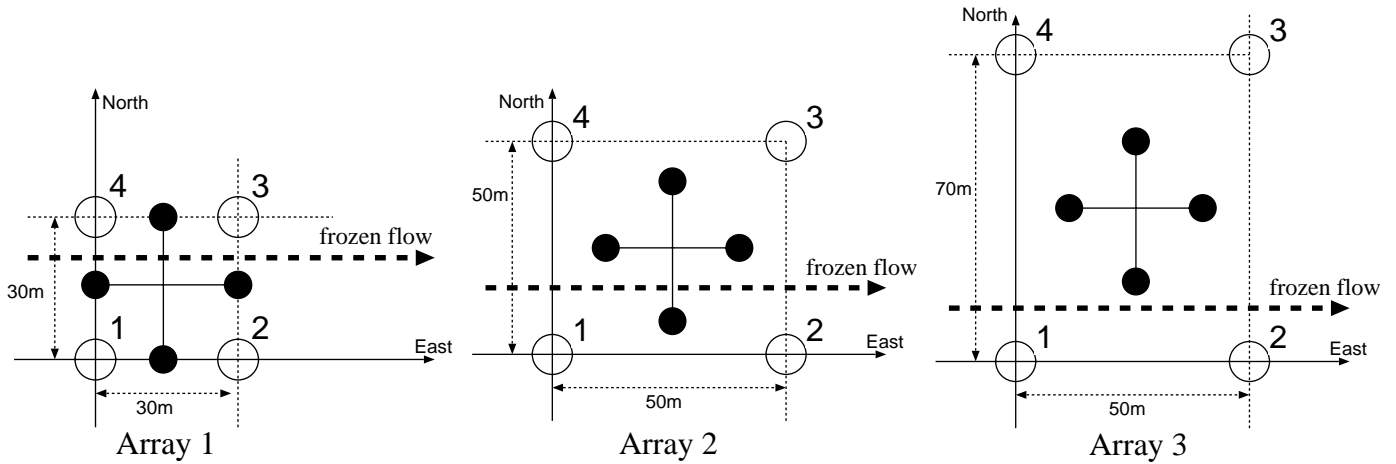


Figure 3: Antenna configurations considered in the simulations. Large open circles represent the 12-m diameter antennas with the WVRs. Small filled circles represent the 7-m diameter antennas of the interferometer array.

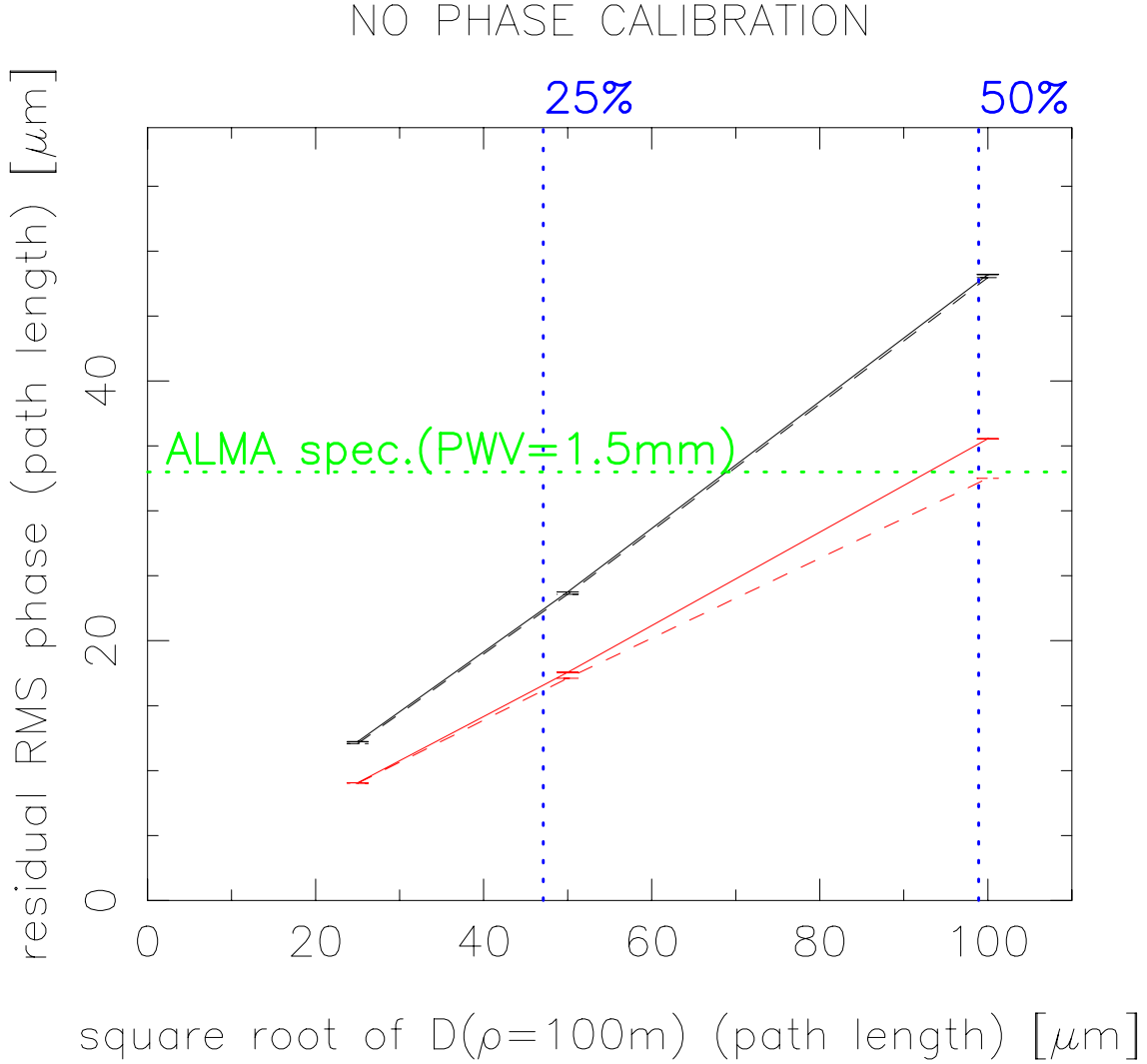


Figure 4: Simulation results of the interferometric residual RMS phase of 30-m baselines without a phase correction. (The so-called natural seeing.) The abscissa is square root of the SSF with a 100-m spatial separation, and the ordinate is the residual RMS phase in path length. Black and red lines represent the structure exponent of 1.16, and 1.67, respectively. Solid and dashed lines represent the wind velocity of 5 and 10 m/s, respectively. A green dotted line represents the ALMA specification in terms of the path length fluctuations ($33 \mu\text{m}$) calculated from $40(1.25 + \text{PWV})$ femto-seconds and $\text{PWV} = 1.5 \text{ mm}$. Blue dotted lines show the 25- and 50-percentile tropospheric conditions (47 and $99 \mu\text{m}$, respectively) estimated from the path length fluctuations of a 300-m spatial separation and an assumption of the structure exponent of 1.16.

4-WVR 2-D SLOPE FITTING

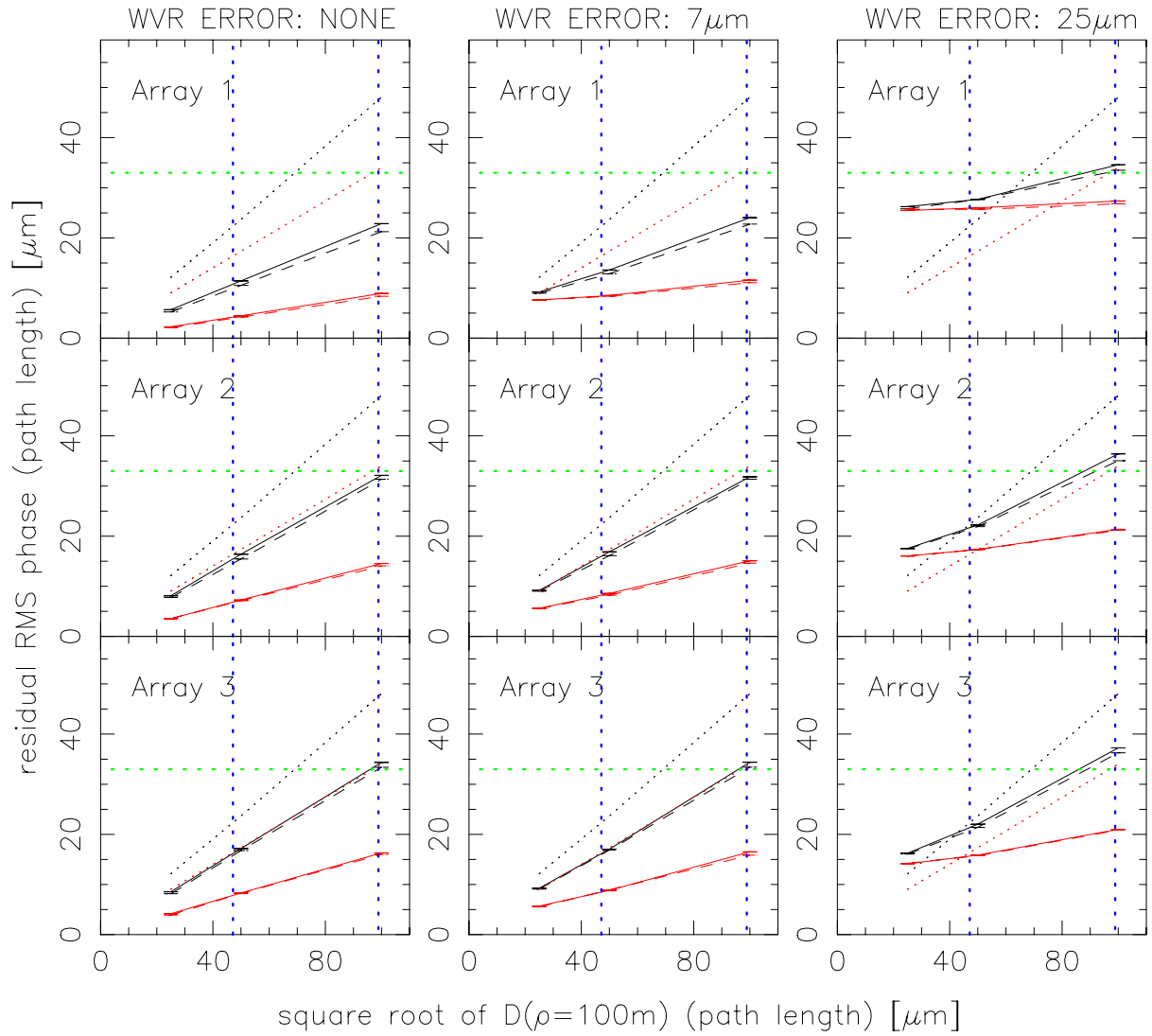


Figure 5: Simulation results of the EPL 2-D slope fitting calibration with WVRs on the four corners. Dotted lines represent the natural seeing already shown in Figure 4.

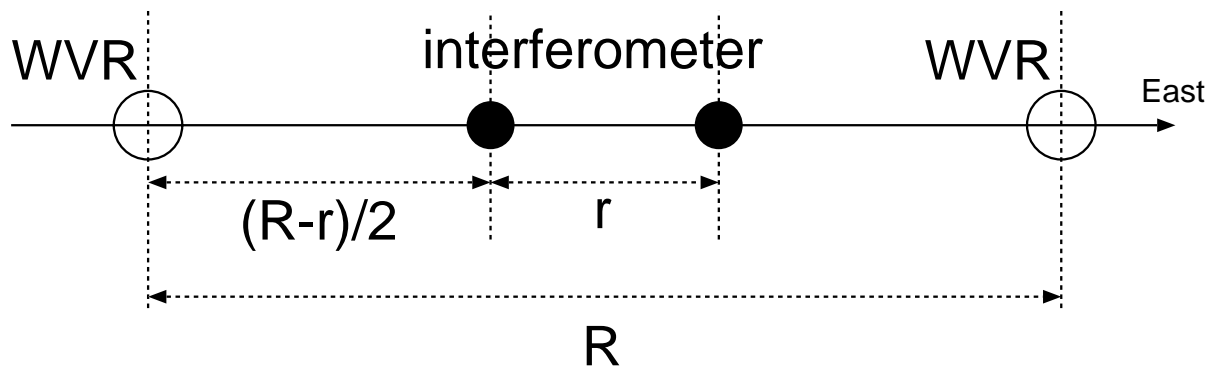


Figure 6: Schematic diagram of a 1-D interferometer for statistical estimations of the proposed phase calibration scheme. Large open and small filled circles represent WVR and interferometer antennas, respectively.

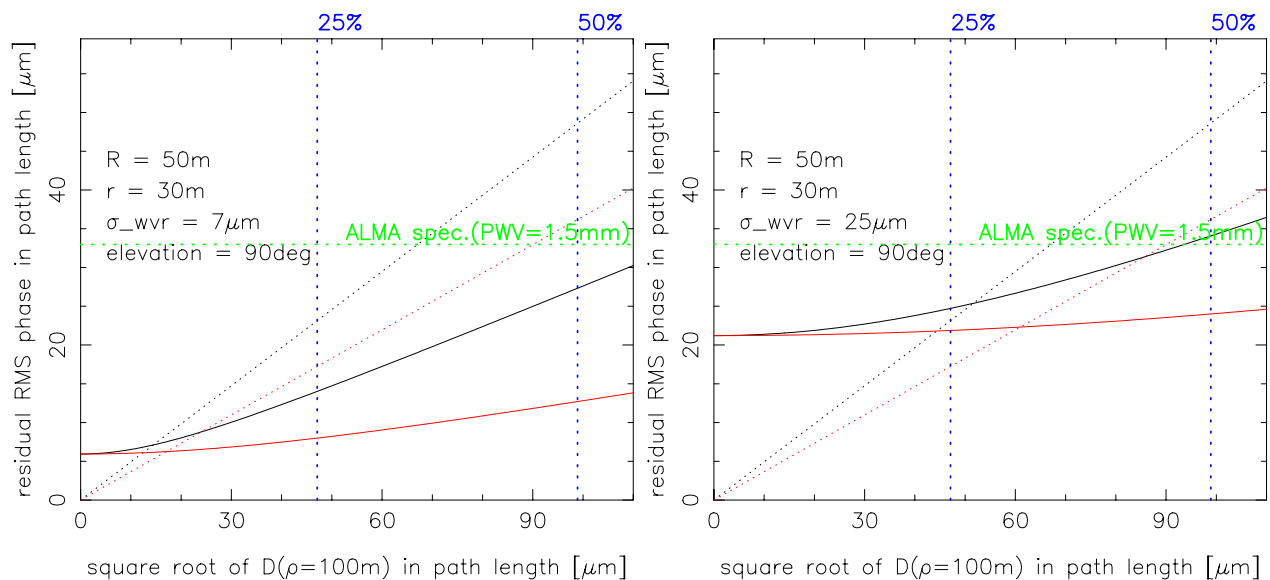


Figure 7: Statistical calculations of the residual RMS phase after the phase correction with the WVR separation of 50 m, and the interferometer baselines of 30 m. The abscissa is square root of the SSF with a 100-m spatial separation, and the ordinate is the residual RMS phase in path length. A black and red line represent the structure exponent of 1.16 and 1.67, respectively. The left and right plots show the case of WVR measurement errors of 7 and 25 μm , respectively.

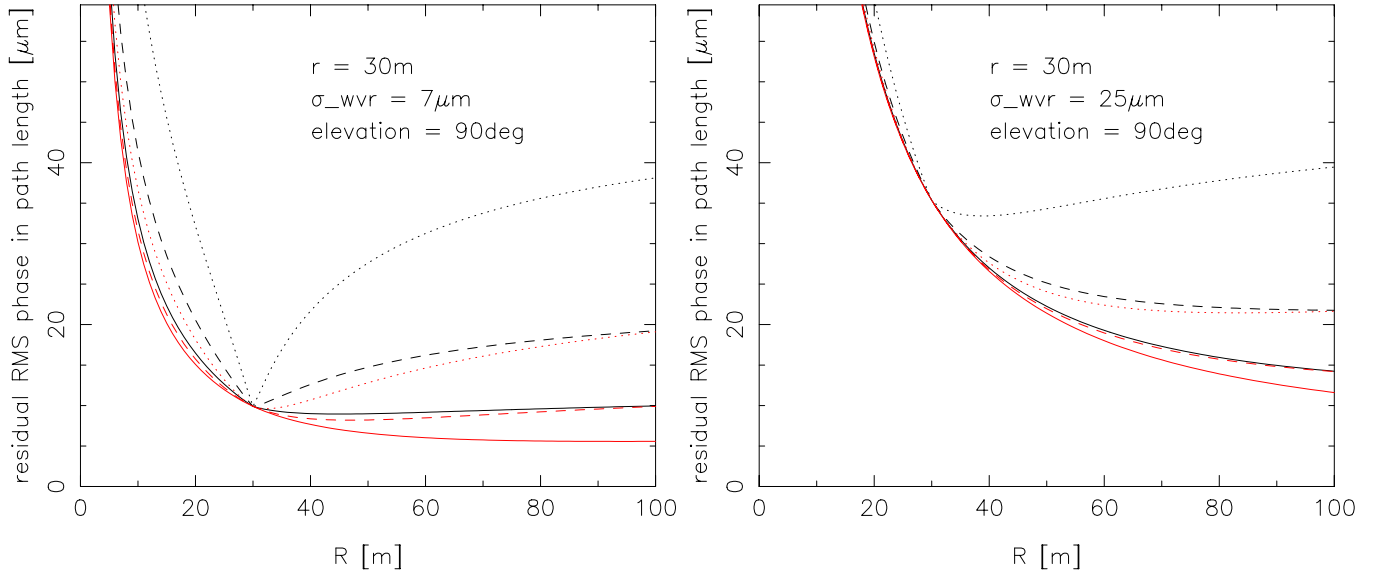


Figure 8: Statistical calculations of the residual RMS phases after the phase correction. The abscissa is a separation between two WVRs, and the ordinate is residual RMS phase in path length. Black and red lines represent the structure exponent of 1.16 and 1.67, respectively. The solid, dashed, and dotted lines represent square root of the SSF with a 100-m spatial separation of 25, 50, and 100 μm , respectively. The left and right plots show the case of WVR measurement errors of 7 and 25 μm , respectively.

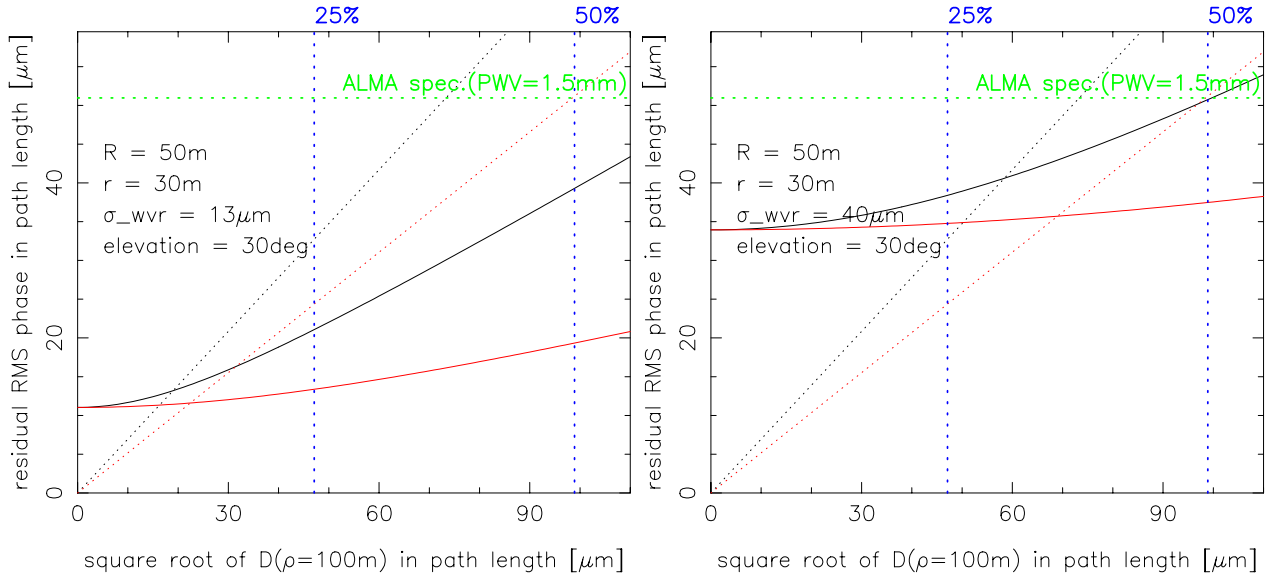


Figure 9: Statistical calculations of the residual RMS phase after the phase correction with the WVR separation of 50 m, and the interferometer baselines of 30 m for observations at an elevation angle of 30° . The ALMA specification in terms of the path length fluctuations ($51 \mu\text{m}$) in the plots is calculated from $40(1.25 + \text{PWV} \cdot \sec Z)$ femto-seconds and $\text{PWV} = 1.5 \text{ mm}$, where Z is the zenith angle (60°). The left and right plots show the case of WVR measurement errors of 13 and $40 \mu\text{m}$, respectively.